Tubeimoside-1 inhibits the proliferation and metastasis by promoting miR-126-5p expression in non-small cell lung cancer cells

HANBING SHI[1], HONGXIA BI[2], XINGYUAN SUN[3], HAIYING DONG[4], YUNFEI JIANG[1], HAIJUN MU[1], WEI LI[1], GUOHUA LIU[1], RUIZHI GAO[2] and JIANG SU[2]

Departments of [1]Respiration II, [2]Respiratory Medicine and [3]Neurology, The Third Affiliated Hospital of Qiqihar Medical University; [4]Laboratory Center of Ultrastructural Pathology, Qiqihar Medical University, Qiqihar, Heilongjiang 161006, P.R. China

Received June 13, 2017; Accepted June 12, 2018

DOI: 10.3892/ol.2018.9051

Abstract. Tubeimoside-1 (TBMS1) possesses broad anticancer activities, including the cytostatic and anti-angiogenesis effects in lung cancer. However, the effect of TBMS1 on the metastasis of non-small cell lung cancer (NSCLC) cells and the potential underlying mechanism remain unclear. In the present study, a cell counting kit-8 assay revealed that TBMS1 suppressed the proliferation of NCI-H1299 cells significantly, particularly following 48 h of treatment. Further studies showed that TBMS1 notably enhanced the apoptosis, and inhibited the migration and invasion of NCI-H1299 cells upon treatment for 48 h. A total of 14 NSCLC tissues and 14 normal adjacent tissues were collected, reverse transcription-quantitative polymerase chain reaction revealed decreased expression of microRNA (miR)-126-5p in NSCLC tissues compared with adjacent NSCLC tissues, which was reversed following TBMS1 administration in NCI-H1299 cells. The overexpression of miR-126-5p induced by TBMS1 was demonstrated to target and downregulate vascular endothelial growth factor (VEGF)-A. Simultaneously, the expression of VEGF-R2 was reduced notably, along with a significant declined in the phosphorylation levels of dual specificity mitogen-activated protein kinase kinase 1 and extracellular signal-regulated kinase (ERK)1/2. Overall, the aforementioned results indicated that TBMS1 inhibited the proliferation and metastasis, and promoted the apoptosis of NCI-H1299 cells, which may be mediated by overexpressing miR-126-5p, which inactivates the VEGF-A/VEGFR2/ERK signaling pathway. Therefore, TBMS1 may be a promising drug for prevention and treatment of NSCLC.

Correspondence to: Professor Jiang Su, Department of Respiratory Medicine, The Third Affiliated Hospital of Qiqihar Medical University, 333 Bukui North Street, Jianhua, Qiqihar, Heilongjiang 161006, P.R. China
E-mail: jiang_su2016@sina.com; jiangsu201629@yeah.net

Key words: non-small cell lung cancer, tubeimoside-1, miR-126-5p, VEGF-A

Introduction

Lung cancer remains the leading cause of cancer-related mortality worldwide with estimated 160,000 death cases/year, and most frequently in developing countries (1). Non-small cell lung cancer (NSCLC) accounts for 85% of the total lung cancer burden and includes the pathologically distinct sub-types: Adenocarcinoma, squamous cell carcinoma and large cell carcinoma (2). Currently, platinum combined with taxanes, vinorelbine, gemcitabine, or pemetrexed are the standard care of advanced NSCLC (3). Despite advances of techniques in diagnosis, staging and surgery and new protocols in chemotherapy and radiotherapy, the overall five-year survival rate of NSCLC is still only about 15% (4). NSCLC cells with strong metastasis capability is capable of evading the regulation in division and apoptosis, which directly leads to treatment failure. Therefore, finding effective therapeutic approaches to inhibit the unlimited proliferation and metastasis of NSCLC cells are expected to reduce mortality of NSCLC.

Bolbostemma paniculatum (Maxim) Franquet (*Cucurbitaceae*) is a traditional Chinese medicinal plant widely used in China for thousands of years for its extensively anti-inflammatory, antiviral and immunosuppressive effects (5). Tubeimoside-1 (TBMS1) is a triterpenoid saponin isolated from the tuber of *Bolbostemma paniculatum* (Maxim) Franquet (6), which sugar chains are connected with 3-hydroxy-3-methyl-glutaric acid to form a unique macro cyclic structure (7). Both *in vivo* and *in vitro* studies reported that TBMS1 exerted potent anti-tumor activity with low toxicity. TBMS1 could suppress proliferation and promote apoptosis in various cancers, including lung cancer (8,9), gastric cancer, liver cancer, nasopharyngeal carcinoma and glioma cancer (5,10-12). TBMS1 also inhibited the migration and invasion of colorectal cancer and breast cancer cells (7,13). Apart from that, Gu *et al* pointed out that TBMS1 suppressed tumor angiogenesis by stimulation of proteasomal VEGFR2 and Tie2 degradation in a NSCLC xenograft model (6). However, neither the roles of TBMS1 in the migration

and invasion of NSCLC cells nor the potential mechanisms of the anti-tumor effects of TBMS1 has been substantiated.

In the present study, NCI-H1299 cells were incubated with 10 μmol/l TBMS1 for different h to evaluate the proliferation and confirm the perfect time, then flow cytometry, wound healing and Transwell invasion assays were employed to explore the effect of TBMS1 on the apoptosis, migration and invasion of NCI-H1299 cells. Further 14 cases of NSCLC tissues and 14 cases of normal adjacent tissues were collected to compare the expression of miR-126-5p in NCI-H1299 cells and tissues with or without TBMS1 administration respectively, then miR-126-5p targeted downstream pathway was detected. We found that the cytostatic and anti-metastatic effects of TBMS1 was associated with overexpression of miR-126-5p repressed VEGF-A/VEGFR2/ERK pathway.

Materials and methods

Cell culture. Human non small cell lung cancer cell line NCI-H1299 was obtained from Shanghai Institutes for Biological Sciences, Chinese Academy of Sciences. Cells were cultured in Roswell Park Memorial Institute-1640 (RPMI-1640; Gibco; Thermo Fisher Scientific, Inc., Waltham, MA, USA) containing 10% fetal bovine serum (FBS; HyClone; GE Healthcare Life Sciences, Logan, UT, USA) and streptomycin/penicillin (100 U/ml) at 37˚C in an atmosphere of 5% CO_2. The suspension was decanted and replaced with fresh medium every 2 to 3 days. When reached 80% confluences, NCI-H1299 cells were digested for subsequent experiments.

Drug treatment. TBMS1 (≥97%; PureOne Biotechnology, Shanghai, China) was dissolved in ddH_2O, and its structure is shown in http://www.pureonebio.com/products/tubeimoside-a-102040-03-9-p588.html. NCI-H1299 cells were exposed to TBMS1 of an ascending concentration range (0, 2.5, 5, 10, 25, 50 μM) for 48 h followed by CCK-8 assay to find the optimum concentration, and incubated with 10 μM TBMS1 for gradient increased h (0, 12, 24, 48 and 72 h) to find the optimum time. For other experiments, NCI-H1299 cells were pre-incubated with 10 μmol/l TBMS1 for 48 h. The untreated cells and 8 μM 5-Fluorouracil (5-FU) treated NCI-H1299 cells were experimented in parallel as positive control.

Patients. We recruited tumor tissues from 14 patients who underwent thoracoscopic lobectomy surgery for non small cell lung cancer between May 2013 and January 2016 at The Third Affiliated Hospital of Qiqihar Medical University, Heilongjiang, China, and 14 paraneoplastic lung tissue samples (>5 cm away from tumors) were taken as healthy control. All tissue specimens were obtained with permission from the Medical Ethics Committee of The Third Affiliated Hospital of Qiqihar Medical University. The median age of all patients was 66.57 years (range, 43-78 years). None of the patients received chemotherapy, radiotherapy or immunotherapy before surgery. The 14 tumor samples were staged according to the 2002 tumor node metastasis (TNM) classification with 0 as non-invasive (pTa), 7 as invasive pT1 and 8 as invasive pT2.

Cell Counting Kit-8 (CCK-8) assay. NCI-H1299 cells were planted in 96-well plates with a density of $1x10^4$ per well and cultured to 80% confluence, followed by incubating with various concentrations of TBMS1 for indicated time, with five replicates for each testing point including the negative control, positive control and blank wells. Thereafter, the cell viability was measured by Enhanced Cell Counting Kit-8 (Beyotime Institute of Biotechnology, Haimen, China) completely following the manufacturer's directions (14-16). Optical density (OD) values were evaluated at 450 nm by a microplate reader (BioTek Instruments, Inc., Winooski, VT, USA).

Hoechst staining. NCI-H1299 cells were inoculated onto coverslips at a density of $5 x10^4$ per well in 12-well plates. When reached to 80% confluences, the suspension was decanted and cells were treated with 10 μM TBMS1 for 48 h. Hoechst staining assay was performed with the Hoechst Staining kit (Beyotime Institute of Biotechnology) following the manufacturer instructions. Briefly, the cells on coverslips were fixed for 20 min using indicated stationary liquid and stained at room temperature for 5 min using a total of 0.5 ml Hoechst 33258 solution with dropwise addition. Then the coverslips were mounted inversely onto slides with indicated anti-fluorescein quencher and observed under a fluorescence microscope (Olympus Corporation, Tokyo, Japan).

Flow cytometric analysis of cell apoptosis. According to the instructions of the Annexin V-FITC/PI apoptosis detection kit (Nanjing KeyGen Biotech Co., Ltd., Nanjing, China), the collected $5x10^5$ cells were resuspended in 500 μl binding buffer, mixed sequentially with 5 μl Annexin V-FITC and 5 μl PI and incubated for 15 min in the dark at room temperature. Cell apoptosis was assessed immediately with flow cytometry and analyzed with CellQuest software (BD Biosciences, Franklin Lakes, NJ, USA).

Wound healing assay. Cells were inoculated in 6-well plates until 80% confluence. A wound was gently created on each cell monolayer by a 200 μl pipette tip and rinsed with a FBS-free RPMI-1640 medium to remove detached cells. Then the cells were grown in FBS free PMI-1640 medium supplemented with or without drug treatment for 48 h, and migrating cells were imaged under an inverted microscope. The migration rate was the ratio of the migrated distance to the initial distance.

Transwell invasion assay. The matrigel-based invasion assay was carried out using a 6-well transwell system (Corning Incorporated, Corning, NY, USA) with a matrigel (BD Biosciences) pre-coated polycarbonate membrane at the upper chamber. The collected cells were resuspended in FBS-free RPMI-1640 medium with or without indicated drug and plated in the upper chamber with a density of $2x10^4$ per well. 700 μl RPMI-1640 containing 10% FBS was added into the lower chamber. After 48 h of incubation, the non-invading cells on the upper surface of the membrane were removed with cotton swabs. The invading cells at the undersurface of the membrane were fixed with 4% paraformaldehyde for 20 min and stained by crystal violet for 5-10 min. The invading cells in each group were calculated in five randomly selected fields under an inverted microscope.

Reverse transcription-quantitative polymerase chain reaction (RT-PCR). Total RNA from tissue samples or NCI-H1299 cells

was extracted by an RNA extraction kit (Tiangen Biotech Co., Ltd., Beijing, China) according to the manufacturer instructions and was reverse-transcribed into cDNA. 2 μl cDNA was amplified with 10 μl Bestar® SybrGreen qPCR masterMix (DBI® Bioscience, Ludwigshafen, Germany), 1 μl primers and 7 μl ddH_2O in an Mx3000P (Agilent Technologies, Inc., Santa Clara, CA, USA) with the following cycling profile: Initial denaturation at 95˚C for 2 min, 40 cycles consisting of 94˚C for 20 sec, 58˚C for 20 sec, and 72˚C for 20 sec. Primer sequences were: miR-126-5p, 5'-CTCAACTGGTGTCGT GGAGTCGGCAATTCAGTTGAGCGCGTA-3' (sense) and 5'-ACACTCCAGCTGGGCATTATTACTTTTGGTA-3' (antisense); miR-29, 5'-CTCAACTGGTGTCGTGGAGTCGGC AATTCAGTTGAGTAACCG-3' (sense) and 5'-ACACTCCAG CTGGGTAGCACCATCTGAAATC-3' (antisense); miR-128, 5'-CTCAACTGGTGTCGTGGAGTCGGCAATTCAGTT GAGTCTCAG-3' (sense) and 5'-ACACTCCAGCTGGGC GGGGCCGTAGCACTGT-3' (antisense); miR-206, 5'-CTC AACTGGTGTCGTGGAGTCGGCAATTCAGTTGAGCCA CAC-3' (sense) and 5'-ACACTCCAGCTGGGTGGAATG TAAGGAAGTG-3' (antisense); VEGFR-A, 5'-AGGGCA GAATCATCACGAAGT-3' (sense) and 5'-AGGGTCTCGATT GGATGGCA-3' (antisense); VEGFR-2, 5'-ATAGAAGGT GCCCAGGAAAAG-3' (sense) and 5'-GTCTTCAGTTCC CCTCCATTG-3' (antisense); MEK1, 5'-GGGCTTCTATGG TGCGTTCTA-3' (sense) and 5'-CCCACGGGAGTTGAC TAGGAT-3' (antisense); ERK, 5'-TCTGGAGCAGTATTA CGACCC-3' (sense) and 5'-CTGGCTGGAATCTAGCAG TCT-3' (antisense); β-actin 5'-ATCGTGCGTGACATTAAG GAGAAG-3' (sense) and 5'-AGGAAGGAAGGCTGGAAG AGTG-3' (antisense); U6, 5'-CTCGCTTCGGCAGCACA-3' (sense) and 5'-AACGCTTCACGAATTTGCGT-3' (antisense). Relative expression was obtained by $2^{-\Delta\Delta CT}$ method. β-actin and U6 were served as internal controls for cells and tissues respectively.

Western blot analysis. Total proteins in NCI-H1299 cells were lysed by NP-40 lysate (Beyotime Institute of Biotechnology) containing 1% phenylmethanesulfonyl fluoride (PMSF). The protein concentration was determined using a bicinchoninic acid (BCA) protein assay kit (Beyotime Institute of Biotechnology). 20 μg proteins in each sample was loaded and separated by SDS-polyacrylamide gel electrophoresis (PAGE) and transferred onto polyvinylidene fluoride (PVDF) membranes (EMD Millipore, Billerica, MA, USA). The blots were then blocked with 5% non-fat milk overnight at 4˚C and incubated at 4˚C overnight with the specific primary antibodies as follows: anti-VEGFR-2, anti-ERK1/2, anti-p-ERK1 (pT202/pY204)+p-ERK2 (pT185/pY187) (all 1:1,500 diluted; Abcam, Cambridge, MA, USA); anti-MEK1, anti-p-MEK1 (pS298) (both 1:1,000 diluted; Abcam). After washed with TBST for three times, the membranes were incubated with a secondary goat anti-rabbit IgG-HRP antibody (1:20,000 diluted; Wuhan Boster Biological Technology, Ltd., Wuhan, China) at 37˚C for 40 min. An enhanced chemiluminescence (ECL; EMD Millipore) detection method was employed to visualize the target bands, and relative protein intensities were analyzed by Gel-Pro-Analyzer software (Media Cybernetics, Rockville, MD, USA). GAPDH was used as an internal control.

Immunofluorescence assay. NCI-H1299 cells were grown on coverslips with appropriate treatment and fixed with 4% formaldehyde for 15 min followed by permeabilized with 0.1% Triton X-100 (Ameresco, Inc., Framingham, MA, USA) for 30 min. After washed three times with PBS, the coverslips were blocked with goat serum (Solarbio, Beijing, China) for 1 h at room temperate. Subsequently, cells were stained with primary antibodies against VEGF-A (1:200 diluted; Abcam) at 4˚C overnight followed by incubated with Cy3-labeled goat anti-rabbit IgG secondary antibody (1:200; Beyotime Institute of Biotechnology) for 1 h at room temperature. Unbound antibodies at each step were washed three times by PBS. Thereafter, cells were stained with 4',6-diamidino-2-phenylindole (DAPI) for 5 min and finally rinsed with PBS. The coverslips were mounted inversely onto slides with neutral gum and observed under a fluorescence microscope.

Statistical analysis. Statistical analysis was carried out by GraphPad Prism v5.0 software (GraphPad Software, Inc., La Jolla, CA, USA). All values except for the clinical data are reported as mean ± standard deviation (SD). Differences between groups in RT-PCR detection of clinical data were calculated with unpaired Student's t-test. Other differences comparison between groups were analyzed with one-way analysis of variance followed by Tukey's Bonferroni post hoc test. $P<0.05$ was considered to indicate a statistically significant difference.

Results

TBMS1 suppresses proliferation and enhances apoptosis of NCI-H1299 cells. To explore the effect of TBMS1 on the survival of NCI-H1299 cells, we conducted CCK-8, Hoechst staining and flow cytometry to detect the proliferation and apoptosis of NCI-H1299 cells with TBMS1 incubation for different h. We found that cell viability exhibited dose-dependent inhibitions after TBMS1 administration for 48 h, and the inhibitory effect was sharply increased at 10 μM TBMS1 treatment, so we chose 10 μM TBMS1 for subsequent experiments ($P<0.001$; Fig. 1A). Moreover, the proliferation of NCI-H1299 cells was inhibited significantly since 10 μM TBMS1 treating for 24 h, and the growth inhibitory rate elevated to the peak between the points of 24 and 48 h treatment ($P<0.001$; Fig. 1B), the inhibition effect at 72 h was not as prominent as at 48 h ($P<0.01$). Hence, we chose 48 h treatment time for subsequent experiments. As shown in Fig. 1C, cells were regular with uniform chromatin in control, but nuclear condensation, fragmentation and apoptotic bodies were appeared in a portion of NCI-H1299 cells administrated with TBMS1 or 5-FU. From flow cytometry assay, the total apoptosis rate was stimulated by 3.78 folds in TBMS1-treated cells compare with control ($P<0.001$; Fig. 1D). The above results demonstrated that TBMS1 suppresses proliferation and enhances apoptosis of NCI-H1299 cells.

TBMS1 inhibits the migration and invasion of NCI-H1299 cells. Wound healing and Transwell invasion assay were employed to address the effect of TBMS1 on the migration and invasion of NCI-H1299 cells. The migration rate of NCI-H1299 cells with TBMS1 treatment was declined by 2.05 folds than control ($P<0.001$; Fig. 2A), and the numbers of invading cells was

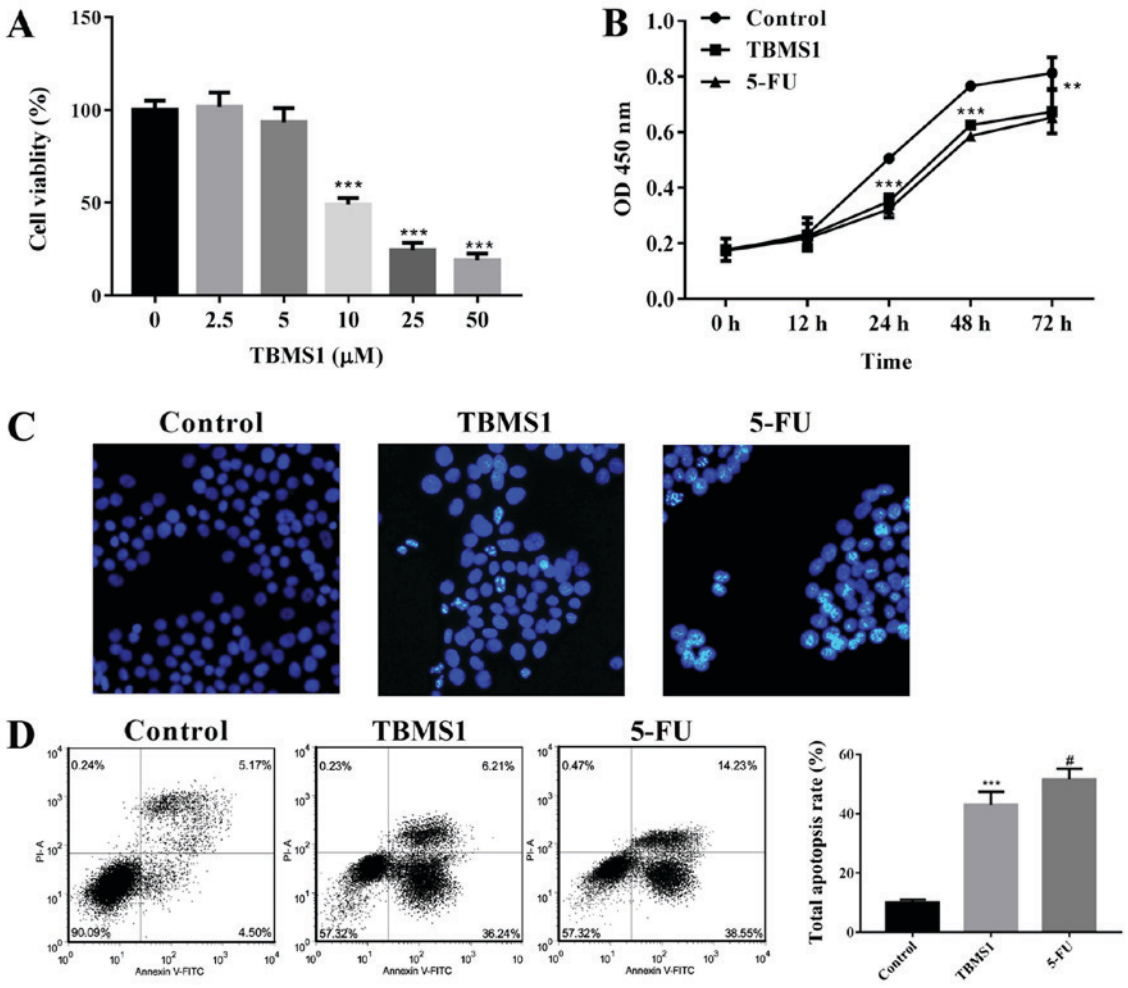

Figure 1. TBMS1 suppresses proliferation and enhances apoptosis of NCI-H1299 cells (A) NCI-H1299 Cells were seeded in 96-well plates and exposed to increased concentrations of TBMS1 (0, 2.5, 5, 10, 25, 50 μM) for 48 h, followed by CCK-8 assay. (B) cells were seeded in 96-well plates and subjected to 10 μmol/l TBMS1 at indicated intervals from 0 up to 72 h, followed by CCK-8 assay. (C) Cells were planted on coverslips and incubated with 10 μmol/l TBMS1 for 48 h, Hoechst staining was employed to detect cell apoptosis. Representative examples of images are shown. Apoptotic cells appeared to be bright white. Magnification, x200. (D) Cell apoptosis was examined by Annexin V-FITC and propidium iodide stained flow cytometry. Cells are characterized as healthy cells (bottom left quadrant), early apoptotic cells (bottom right quadrant), necrotic cells (top left quadrant) and late apoptotic cells (top right quadrant), and the total apoptosis rate is calculated on the right. Above experiments were performed for three times. Non-TBMS1 treated control was used as negative control, and 5-FU treated cells was served as positive control. Data are expressed as mean ± SD. Compared with non-TBMS1 treated control, **P<0.01, and ***P<0.001; compared with 5-FU treated cells, $^{\#}$P<0.05. TBMS1, Tubeimoside-1.

28.80±3.40, which was remarkably decreased compared with control cells (85.76±8.23) (P<0.001; Fig. 2B), indicating that TBMS1 inhibits the migration and invasion of NCI-H1299 cells.

TBMS1 increases the expression of miR-126-5p. According to Ricciuti *et al* (17), we chose miR-29, miR-206, miR-126-5p and miR-128, which are all downregulated in NSCLC and play roles in inhibiting cell growth, migration and invasion, to compare their expressions with or without TBMS1 administration in NSCLC tissues and NCI-H1299 cells. First, we collected 14 cases of pathological specimens from patients with NSCLC and 14 cases of normal adjacent tissues for RT-PCR detection. We found that the expression level of miR-29, miR-206, miR-126-5p and miR-128 were all notably reduced in NSCLC tissues, while the downregulated expressions of miR-29 and miR-126-5p were particularly significant (P<0.05; Fig. 3A-D). Next, although miR-29 and miR-126-5p were both apparently upregulated in NCI-H1299 cells upon TBMS1 treatment for 48 h compared with control, TBMS1 treatment, the increased level of miR-126-5p in NCI-H1299 cells following TBMS1 treatment was much higher than 5-FU treatment (P<0.001; Fig. 3E-H). So we selected miR-126-5p for subsequent expremements. These results demonstrated that TBMS1 could increase the expression of miR-126-5p in NCI-H1299 cells.

TBMS1 downregulates the expression of miR-126-5p-targeted VEGF-A. It is a well establish fact that VEGF-A is one of the target genes of miR-126-5p (Fig. 4A), so we carried out RT-PCR and immunofluorescence assay to evaluate the expression of VEGF-A in TBMS1-treated NCI-H1299 cells. Compared with non-TBMS1 treated control cells, the expression of VEGF-A was decreased significantly at both mRNA and protein levels (Fig. 4B and C), suggesting that TBMS1 induced overexpressing miR-126-5p directly downregulates VEGF-A level in NCI-H1299 cells.

TBMS1 inactivates VEGFR2 mediated ERK pathway. To identify the alteration of VEGFR-2 mediated ERK pathway, we

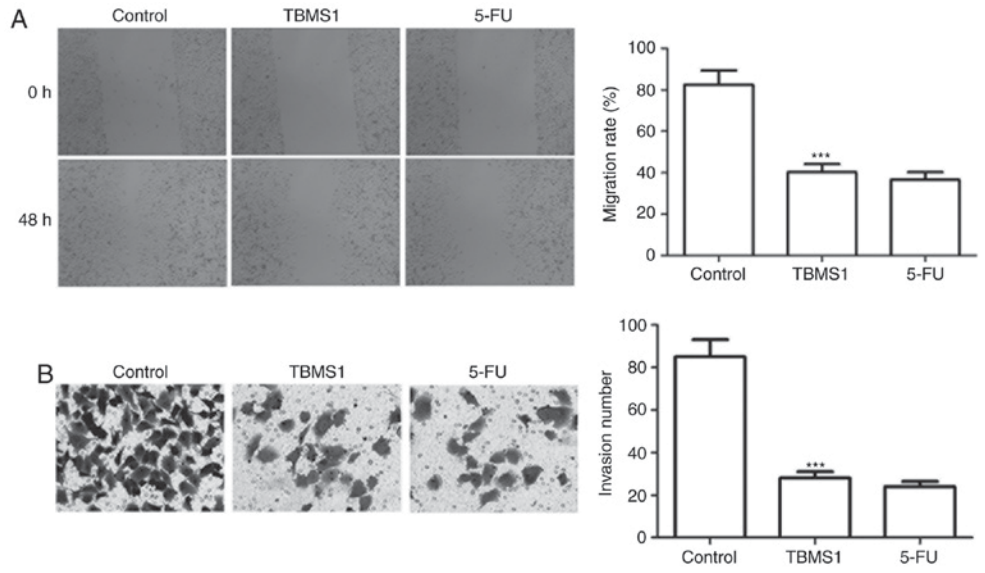

Figure 2. TBMS1 inhibits the migration and invasion of NCI-H1299 cells (A) Cells were inoculated in 6-well plates, and wound healing assay was performed with or without indicated drug treatment for 48 h. Migration rate was calculated and presented as a bar chart. (B) Cellular invasion was assessed with a Transwell system. After incubated for 48 h with or without indicated drug, invading cells were fixed and stained with crystal violet. The above two experiments were done in triplicates for statistical significance, and the representative images are shown. Magnification, x200. Data are given as mean ± SD, compared with control, ***P<0.001. TBMS1, Tubeimoside-1.

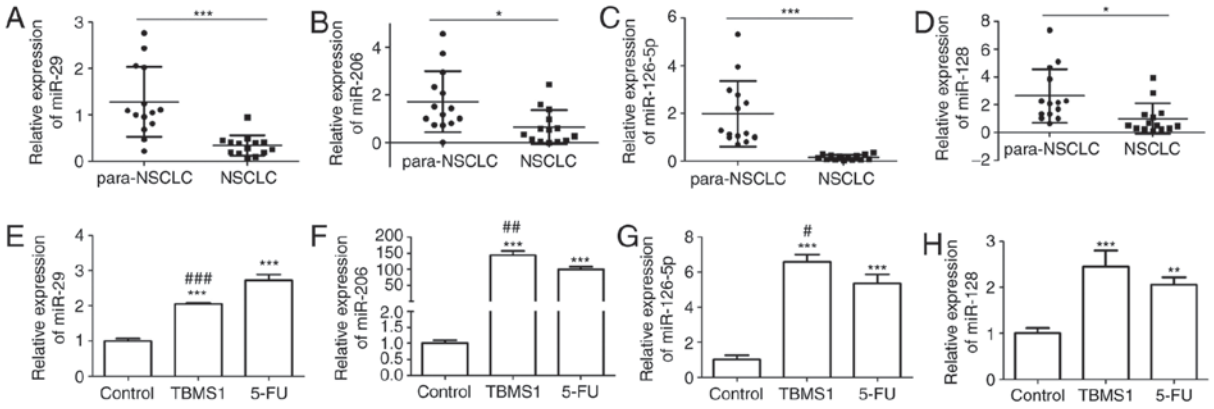

Figure 3. TBMS1 increases the expression of miR-126-5p RT-PCR analysis of miR-29 (A), miR-206 (B), miR-126-5p (C) and miR-128 (D) expression levels in NSCLC tissues and paraneoplastic tissues. U6 was served as an internal control, compared with para-NSCLC, *P<0.05 and ***P<0.001. RT-PCR analysis of miR-29 (E), miR-206 (F), miR-126-5p (G) and miR-128 (H) expression levels in NCI-H1299 cells with or without indicated drug incubation for 48 h, which data are presented as mean ± SD, and β-actin was used as an internal control, compared with control, **P<0.01, ***P<0.001; compared with 5-FU, $^{\#}$P<0.05, $^{\#\#}$P<0.01 and $^{\#\#\#}$P<0.001. The above experiments were repeated three times. TBMS1, Tubeimoside-1; NSCLC, non-small cell lung cancer.

performed RT-PCR and western blot to detect the expression or phosphorylation of VEGFR-2, MEK1 and ERK1/2. The mRNA and protein levels of VGFR-2 in NCI-H1299 cells incubated with TBMS1 for 48 h were 2.28-fold and 2.0-fold lower than those in the respective control cells (P<0.001; Fig. 5A and B). Moreover, the expression of MEK1 and ERK were both sharply reduced at mRNA levels in comparison with control (P<0.001; Fig. 5A). At the same time, the phosphorylation level of MEK1 and ERK1/2 were both decreased significantly (P<0.001; Fig. 5B). Taken together, TBMS1 inactivates VEGFR2 mediated ERK pathway in NCI-H1299 cells.

Discussion

Previous researches revealed the cytostatic and pro-apoptotic effects of TBMS1 in multiple cancer cells, including lung cancer (8,9). But less is known about the internal event of NSCLC cells during the anti-tumor effects of TBMS1. Our study confirmed that TBMS1 suppressed the proliferation, migration and invasion, boosted the apoptosis of NCI-H1299 cells through overexpressing miR-126-5p, subsequently resulted in the inhibition of VEGF-A/VEGFR2/ERK pathway.

Hao *et al* (8) and Lin *et al* (9), both identified that TBMS1 could inhibit growth and induce apoptosis in lung cancer cells, which was basically consistent with our study using NCI-H1299 cell line. NCI-H1299 cell line originates from a lymph node metastasis in patients with NSCLC and accepted early radiotherapy. The most obvious feature of NCI-H1299 is its absence of pro-apoptotic p53 expression. Singla *et al* (18) and Wu *et al* (19) have demonstrated the possibility of metastasis induced by NCI-H1299 cells in mice model. In this study, we showed that TBMS1 blocked the migration and

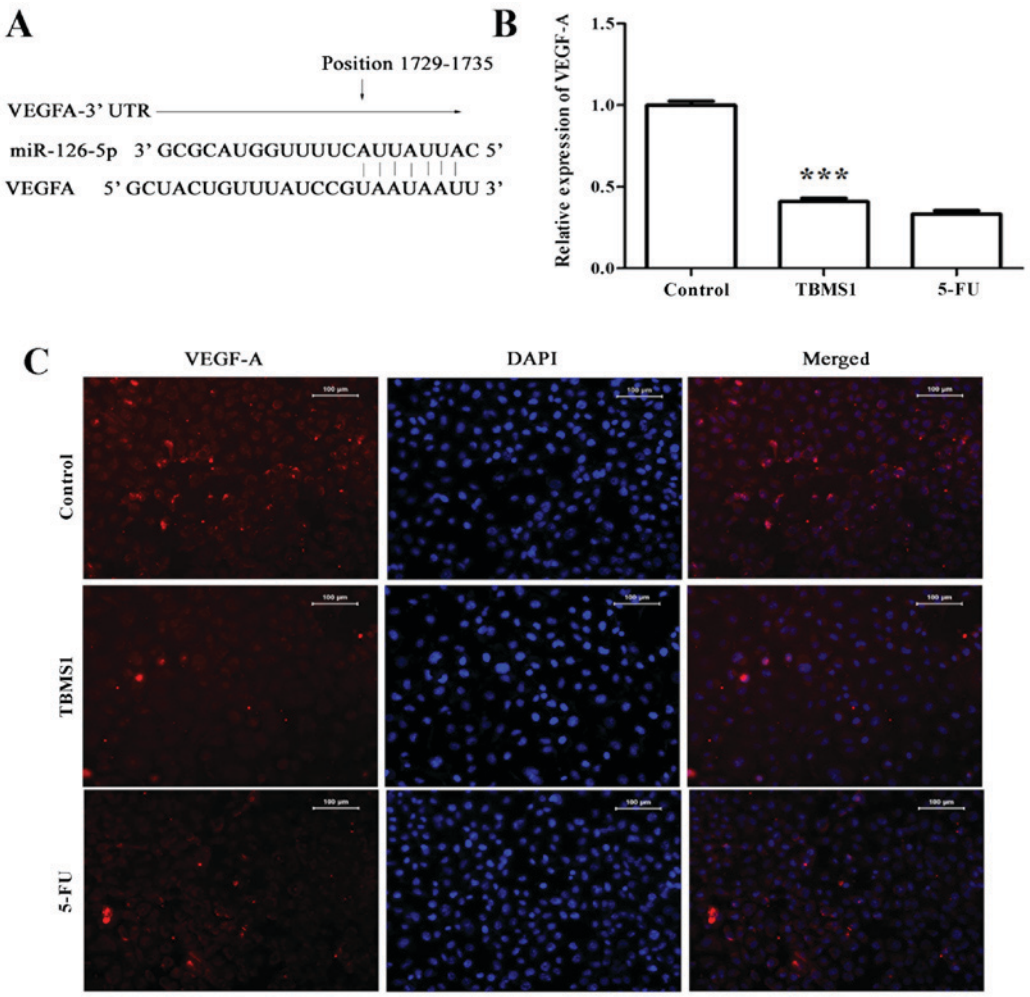

Figure 4. TBMS1 downregulates the expression of miR-126-5p-targeted VEGF-A (A) The 3'UTR sequence of VEGF-A and its binding site on miR-126-5p. (B) RT-PCR detection of VEGF-A mRNA expression in TBMS1-treated NCI-H1299 cells. Data in each group are expressed as mean ± SD from three independent experiments. β-actin was used as an internal control. Compared with control, $^{***}P<0.001$. (C) Detection on the expression of VEGF-A by immunofluorescence staining under x200 magnification (scale bar: 100 μm). Representative photomicrographs from repeated experiments are shown. VEGF-A was visualized with Cy3-labeled goat anti-rabbit IgG as bright white. TBMS1, Tubeimoside-1.

invasion of NCI-H1299 cells significantly, first indicating the anti-metastatic effect of TBMS1 in NSCLC cells.

The pre-miR-126, located in the epidermal growth factor-like domain 7 (EGFL7) gene, produces two mature miRNA chains, miR-126-3p (referring to the 3' part of the miR-126 transcript) and miR-126-5p (referring to the 5' part of the miR-126 transcript, also called miR-126*) (20). Shibayama *et al* (21), proved that upregulation of miR-126-5p was associated with drug resistance to cytarabine and poor prognosis in acute myeloid leukemia (AML) patients. Further studies reported that miR-126-5p acted as a tumor suppressor in many tumors such as prostate cancer, melanoma and breast cancer, as evidenced by repressing the proliferation and invasion of cancer cells (22-26). Clinical researches revealed that miR-126-5p was notably downregulated in lung cancer patients (26). Similarly, miR-126-5p was remarkably downregulated in the tissues we recruited from NSCLC patients compared with control, but the expression of miR-126-5p was raised much higher after TBMS1 administration in NCI-H1299 cells, suggesting that TBMS1 inhibited the proliferation and metastasis through increasing the expression miR-126-5p in NSCLC cells.

Vascular endothelial growth factor-A (VEGF-A), an important member of VEGF family, is upregulated in multiple malignant tumors, such as cancers of breast, lung, brain, pancreas, ovarian, kidney and bladder, which presents highly correlation with staging, pathological grading and a poor prognosis (27-32). Besides its essential role in regulating physiologic and pathologic angiogenesis, VEGF-A also triggers the growth, survival, and migration of cancer cells (33). Prior studies proved that VEGF-A is one of the target genes of miR-126-5p (34). Tang *et al* (35), pointed out that decreased expression of miR-126-5p upregulated VEGF-A and contributed to lipopolysaccharide-induced acute lung injury. Liu *et al* (34), demonstrated that downregulated VEGF by miR-126 could inhibit the proliferation of lung cancer cells. In this study, we showed the significantly reduced mRNA and protein VEGF-A levels in TBMS1 treated NCI-H1299 cells, indicating that the increased miR-126-5p expression targets VEGF-A, which may be associated with the anti-tumor effect of TBMS1.

VEGF-A mediates its activity mainly via 2 receptor tyrosine kinases (RTKs): VEGF receptor 1 (VEGFR-1) and VEGF receptor 2 (VEGFR-2). VEGFR-2 is the most

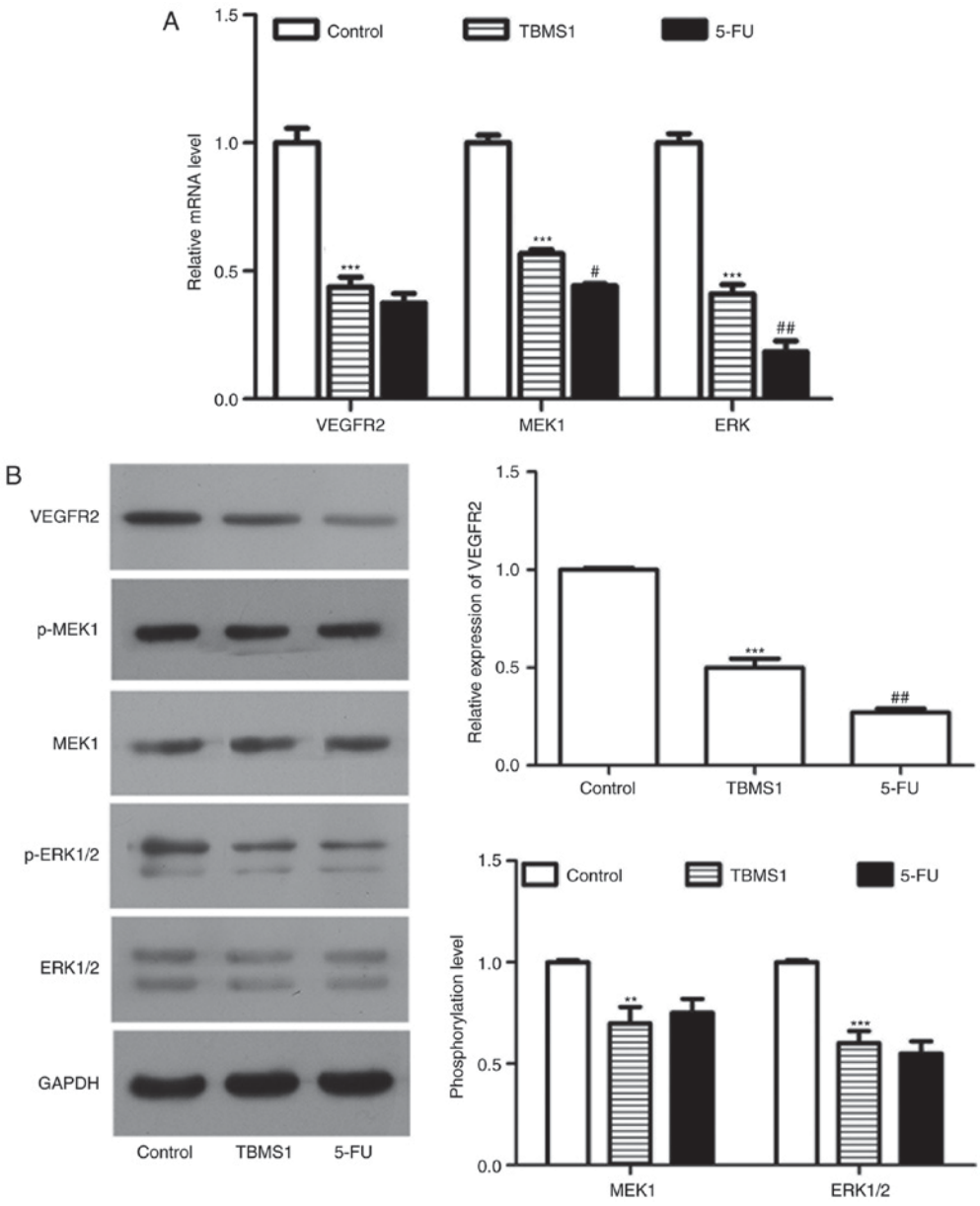

Figure 5. TBMS1 inactivates VEGFR2 mediated ERK pathway. (A) RT-PCR analysis of VEGFR-2, MEK1 and ERK mRNA expression levels. β-actin was used as an internal control. (B) Western blot analysis on VEGFR-2 protein expression and MEK1 and ERK1/2 phosphorylation levels. GADPH was served as an internal control. Representative blots are presented with corresponding densitometric analysis is shown. Data are given as mean ± SD from three independent experiments. Compared with control, **P<0.01, and ***P<0.001; compared with 5-FU, $^{\#}$P<0.05, $^{\#\#}$P<0.01. TBMS1, Tubeimoside-1.

biologically responsible for cell proliferation and migration (36). Extracellular signal regulated kinase (ERK)1/2 pathway belongs to MAPKs pathway that are highly conserved three stage kinase cascade amplification pathway models from yeast to mammals. ERK1/2 pathway is generally described as Ras-Raf-MEK-ERK1/2 model. Activated ERKs translocates into nucleus and stimulates multiple transcription factors to promote the expression of related genes in mitotic G0/G1 phase (37). Santos *et al* (38), found a strong pro-apoptotic effect of the intracellular VEGFR-2 inhibitor through inhibiting ERK1/2 pathway. Furthermore, overexpression of VEGF-A augmented cell migration and invasion through VEGF-A/VEGFR2/MEK/ERK1/2 signaling (39). Our experiment showed the significant downregulation of VEGFR-2 and an apparently inhibitory of the activation of ERK1/2 pathway upon TBMS1 administration. We therefore speculate that TBMS1 suppresses the proliferation, migration and invasion and promotes the apoptosis of NCI-H1299 cells through overexpressing miR-126-5p, which ultimately reduces VEGF-A/VEGFR-2/ERK1/2 pathway.

In summary, our present study revealed the cytostatic and anti-metastatic effects of TBMS1, which may induced by TBMS1 increased miR-126-5p expression and subsequent inactivated VEGF-A/VEGFR-2/ERK1/2 pathway in NCI-H1299 cells. Our data preliminarily identified the significant roles of TBMS1 and the potential mechanism *in vitro*. TBMS1 may become a promising candidate for NSCLC therapy.

Acknowledgements

Not applicable.

Funding

No funding was received.

Availability of data and materials

The authors declare that all available data is presented in this submitted article.

Authors' contributions

HBS, HXB and JS conceived and designed the study. HBS, HXB, XYS, HYD, YFJ, HJM, WL, GHL and RZG performed the experiments. HBS and JS wrote the paper. All authors read and approved the manuscript.

Ethics approval and consent to participate

All tissue specimens were obtained with permission from the Medical Ethics Committee of The Third Affiliated Hospital of Qiqihar Medical University. All participants have read and signed the written informed consent.

Consent for publication

All participants have read and signed the written informed consent for the publication.

Competing interests

The authors declare that they have no competing interests.

References

1. National Lung Screening Trial Research Team, Aberle DR, Adams AM, Berg CD, Black WC, Clapp JD, Fagerstrom RM, Gareen IF, Gatsonis C, Marcus PM and Sicks JD: Reduced lung-cancer mortality with low-dose computed tomographic screening. N Engl J Med 365: 395-409, 2011.
2. Minguet J, Smith KH and Bramlage P: Targeted therapies for treatment of non-small cell lung cancer-Recent advances and future perspectives. Int J Cancer 138: 2549-2561, 2016.
3. Villaruz LC and Socinski MA: Is there a role of nab-paclitaxel in the treatment of advanced non-small cell lung cancer? The data suggest yes. Eur J Cancer 56: 162-171, 2016.
4. Siegel R, Naishadham D and Jemal A: Cancer statistics, 2012. CA A Cancer J Clin 62: 10-29, 2012.
5. Yin Y, Chen W, Tang C, Ding H, Jang J, Weng M, Cai Y and Zou G: NF-kB, JNK and p53 pathways are involved in tubeimoside-1-induced apoptosis in HepG2 cells with oxidative stress and G (2)/M cell cycle arrest. Food Chem Toxicol 49: 3046-3054, 2011.
6. Gu Y, Korbel C, Scheuer C, Nenicu A, Menger MD and Laschke MW: Tubeimoside-1 suppresses tumor angiogenesis by stimulation of proteasomal VEGFR2 and Tie2 degradation in a non-small cell lung cancer xenograft model. Oncotarget 7: 5258-5272, 2016.
7. Bian Q, Liu P, Gu J and Song B: Tubeimoside-1 inhibits the growth and invasion of colorectal cancer cells through the Wnt/β-catenin signaling pathway. Int J Clin 8: 12517-12524, 2015.
8. Hao W, Wang S and Zhou Z: Tubeimoside-1 (TBMS1) inhibits lung cancer cell growth and induces cells apoptosis through activation of MAPK-JNK pathway. Int J Clin Exp Pathol 8: 12075-12083, 2015.
9. Lin Y, Xie G, Xia J, Su D, Liu J, Jiang F and Xu Y: TBMS1 exerts its cytotoxicity in NCI-H460 lung cancer cells through nucleolar stress-induced p53/MDM2-dependent mechanism, a quantitative proteomics study. Biochim Biophys Acta 1864: 204-210, 2016.
10. Jia G, Wang Q, Wang R, Deng D, Xue L, Shao N, Zhang Y, Xia X, Zhi F and Yang Y: Tubeimoside-1 induces glioma apoptosis through regulation of Bax/Bcl-2 and the ROS/Cytochrome C/Caspase-3 pathway. Onco Targets Ther 8: 303-311, 2015.
11. Zhang Y, Xu XM, Zhang M, Qu D, Niu HY, Bai X, Kan L and He P: Effects of tubeimoside-1 on the proliferation and apoptosis of BGC823 gastric cancer cells in vitro. Oncol Lett 5: 801-804, 2013.
12. Weng XY, Ma RD and Yu LJ: Apoptosis of human nasopharyngeal carcinoma CNE-2Z cells induced by tubeimoside I. Ai Zheng 22: 806-811, 2003.
13. Peng Y, Zhong Y and Li G: Tubeimoside-1 suppresses breast cancer metastasis through downregulation of CXCR4 chemokine receptor expression. BMB Rep 49: 502-507, 2016.
14. Ni N, Zhang D, Xie Q, Chen J, Wang Z, Deng Y, Wen X, Zhu M, Ji J, Fan X, *et al*: Effects of let-7b and TLX on the proliferation and differentiation of retinal progenitor cells in vitro. Sci Rep 4: 6671, 2014.
15. Lu M, Sun L, Zhou J, Zhao Y and Deng X: Dihydroartemisinin-induced apoptosis is associated with inhibition of sarco/endoplasmic reticulum calcium ATPase activity in colorectal cancer. Cell Biochem Biophys 73: 137-145, 2015.
16. Shan S, Lv Q, Zhao Y, Liu C, Sun Y, Xi K, Xiao J and Li C: Wnt/β-catenin pathway is required for epithelial to mesenchymal transition in CXCL12 over expressed breast cancer cells. Int J Clin Exp Pathol 8: 12357-12367, 2015.
17. Ricciuti B, Mecca C, Crino L, Baglivo S, Cenci M and Metro G: Non-coding RNAs in lung cancer. Oncoscience 1: 674-705, 2014.
18. Singla AK, Downey CM, Bebb GD and Jirik FR: Characterization of a murine model of metastatic human non-small cell lung cancer and effect of CXCR4 inhibition on the growth of metastases. Oncoscience 2: 263-271, 2015.
19. Wu W, Bi C, Credille KM, Manro JR, Peek VL, Donoho GP, Yan L, Wijsman JA, Yan SB and Walgren RA: Inhibition of tumor growth and metastasis in non-small cell lung cancer by LY2801653, an inhibitor of several oncokinases, including MET. Clin Cancer Res 19: 5699-5710, 2013.
20. Meister J and Schmidt MH: miR-126 and miR-126*: New players in cancer. Sci World J 10: 2090-2100, 2010.
21. Shibayama Y, Kondo T, Ohya H, Fujisawa S, Teshima T and Iseki K: Upregulation of microRNA-126-5p is associated with drug resistance to cytarabine and poor prognosis in AML patients. Oncol Rep 33: 2176-2182, 2015.
22. Musiyenko A, Bitko V and Barik S: Ectopic expression of miR-126*, an intronic product of the vascular endothelial EGF-like 7 gene, regulates prostein translation and invasiveness of prostate cancer LNCaP cells. J Mol Med (Berl) 86: 313-322, 2008.
23. Felli N, Felicetti F, Lustri AM, Errico MC, Bottero L, Cannistraci A, De Feo A, Petrini M, Pedini F, Biffoni M, *et al*: miR-126&126* restored expressions play a tumor suppressor role by directly regulating ADAM9 and MMP7 in melanoma. PLoS One 8: e56824, 2013.
24. Zhang Y, Yang P, Sun T, Li D, Xu X, Rui Y, Li C, Chong M, Ibrahim T, Mercatali L, *et al*: miR-126 and miR-126* repress recruitment of mesenchymal stem cells and inflammatory monocytes to inhibit breast cancer metastasis. Nat Cell Biol 15: 284-294, 2013.
25. Sanfiorenzo C, Ilie MI, Belaid A, Barlési F, Mouroux J, Marquette CH, Brest P and Hofman P: Two panels of plasma microRNAs as non-invasive biomarkers for prediction of recurrence in resectable NSCLC. PLoS One 8: e54596, 2013.
26. Vosa U, Vooder T, Kolde R, Vilo J, Metspalu A and Annilo T: Meta-analysis of microRNA expression in lung cancer. Int J Cancer 132: 2884-2893, 2013.
27. Yoshiji H, Gomez DE, Shibuya M and Thorgeirsson UP: Expression of vascular endothelial growth factor, its receptor and other angiogenic factors in human breast cancer. Cancer Res 56: 2013-2016, 1996.
28. Volm M, Koomägi R and Mattern J: Prognostic value of vascular endothelial growth factor and its receptor Flt-1 in squamous cell lung cancer. Int J Cancer 74: 64-68, 1997.
29. Hatva E, Kaipainen A, Mentula P, Jääskeläinen J, Paetau A, Haltia M and Alitalo K: Expression of endothelial cell-specific receptor tyrosine kinases and growth factors in human brain tumors. Ame J Pathol 146: 368-378, 1995.
30. Ellis LM, Takahashi Y, Fenoglio CJ, Cleary KR, Bucana CD and Evans DB: Vessel counts and vascular endothelial growth factor expression in pancreatic adenocarcinoma. Eur J Cancer 34: 337-340, 1998.

31. Boocock CA, Charnock-Jones DS, Sharkey AM, McLaren J, Barker PJ, Wright KA, Twentyman PR and Smith SK: Expression of vascular endothelial growth factor and its receptors flt and KDR in ovarian carcinoma. J Natil Cancer Inst 87: 506-516, 1995.
32. Brown LF, Berse B, Jackman RW, Tognazzi K, Manseau EJ, Dvorak HF and Senger DR: Increased expression of vascular permeability factor (vascular endothelial growth factor) and its receptors in kidney and bladder carcinomas. Am J Pathol 143: 1255-1262, 1993.
33. Ferrara N and Davis-Smyth T: The biology of vascular endothelial growth factor. Endocr Rev 18: 4-25, 1997.
34. Liu B, Peng XC, Zheng XL, Wang J and Qin YW: MiR-126 restoration down-regulate VEGF and inhibit the growth of lung cancer cell lines in vitro and in vivo. Lung Cancer 66: 169-175, 2009.
35. Tang R, Pei L, Bai T and Wang J: Down-regulation of microRNA-126-5p contributes to overexpression of VEGFA in lipopolysaccharide-induced acute lung injury. Biotechnol Lett 38: 1277-1284, 2016.
36. Matsumoto K and Ema M: Roles of VEGF-A signalling in development, regeneration and tumours. J Biochem 156: 1-10, 2014.
37. Zhang W and Liu HT: MAPK signal pathways in the regulation of cell proliferation in mammalian cells. Cell Res 12: 9-18, 2002.
38. Santos SC and Dias S: Internal and external autocrine VEGF/KDR loops regulate survival of subsets of acute leukemia through distinct signaling pathways. Blood 103: 3883-3889, 2004.
39. Tian Y, Xie Q, Tian Y, Liu Y, Huang Z, Fan C, Hou B, Sun D, Yao K and Chen T: Radioactive ^{125}I seed inhibits the cell growth, migration and invasion of nasopharyngeal carcinoma by triggering DNA damage and inactivating VEGF-A/ERK signaling. PLoS One 8: e74038, 2013.